Top seal efficiency of the Lakes Entrance formation, Gippsland Basin: some constraints from seismic inversion and attributes

Laurent Langhi
CSIRO
26 Dick Perry Av, Kensington, WA
laurent.langhi@csiro.au

Bozkurt Ciftci
CSIRO
26 Dick Perry Av, Kensington, WA
bozkurt.ciftci@csiro.au

Dariush Nadri
CSIRO
26 Dick Perry Av, Kensington, WA
dariush.nadri@csiro.au

Louise Goldie Divko
VicDPI
55 Collins St, Melbourne, VIC
louise.goldie-divko@dpi.vic.gov.au

Peter Tingate
VicDPI
55 Collins St, Melbourne, VIC
Peter.Tingate@dpi.vic.gov.au

SUMMARY

The Gippsland Basin is a potential site for CO_2 storage which is dependent on the regional top seal in providing a secure subsurface containment. We present here some geological parameters derived with the aid of seismic attributes and inversion from 2D and 3D reflection seismic surveys predominantly along the southern flank of the basin. These parameters are potentially influential on the top seal efficiency and CO_2 containment security in the basin.

An important factor in top seal efficiency is the spatial variation of its shale content (V_{sh}). The empirical relationship between acoustic impedance and shale content was used to estimate V_{sh}. Composite seismic amplitude and acoustic impedance traces were constructed to establish a tie with the well-derived reference V_{sh}. Using a multi-attribute regression analysis, a transformation was established from seismic attributes and impedance to V_{sh} and used to define V_{sh} pseudo-traces. Eight vertical profiles were produced in the Southern flank of the basin and the V_{sh} data were interpolated to reveal the first order variation in shale content for the top seal.

Equally important in the assessment of containment risk is the distribution and density of faults in top seal. Seismic spectral blueing and attributes were used to increase the resolution of the 2D seismic data and a meta-attribute that sharpens the faults and suppresses non-fault discontinuities was coupled with similarity attributes to ensure a better imaging of low-displacement faults (<20m). Automated mapping of the faults provided fracture density maps which depict the intensely deformed areas with potentially decreased seal efficiency on the southern flank of the basin.

Key words: Gippsland, top seal, faults, integrity, seismic attribute, seismic inversion

INTRODUCTION

The Gippsland Basin is a prolific hydrocarbon province in Victoria and the oldest oil and gas producing offshore area of Australia. The basin also includes substantial brown coal deposits in Latrobe Valley, mining of which is regarded as a critical input to low-cost power generation and sustainable development of Victoria. However, the increasing long-term use of the fossil fuels will be contingent upon a reduction in the emitted green house gases and geological carbon storage is considered as a key mitigation strategy to minimize the release of CO_2 into the atmosphere. As the production of hydrocarbon fields is still strong in the basin, the Victorian Department of Primary Industries is carrying out detailed geological assessments to evaluate the basin's potential beyond the oil and gas fields as a possible sink for large sources of CO_2.

The study area (Figure 1) covers three carbon storage permits, released in 2009 by the Federal Government, located on the southern flank of the Gippsland Basin, predominantly covering the Southern Platform and the Southern Terrace. The Foster and Darriman fault systems bound and separate these two major structural compartments. The study area was surveyed by a recent (2010) 2D seismic program but also possess vintage 2D surveys and a 3D mega survey predominantly on the Central Deep but partially extending to the study area (Figure 1C).

In the Gippsland Basin the Late Oligocene – Early Miocene Lakes Entrance Formation shows potential as a low permeability regional barrier to vertical fluid flow and possesses seal potential suitable for subsurface containment of significant volumes of CO_2 (Goldie-Divko et al., 2010) (Figure 2A). The seal potential is reported to be excellent in the Central Deep, western Northern Terrace and the onshore Lake Wellington Depression and good over the Southern Terrace and Platform. However, the Lakes Entrance Formation is faulted in places and the related strain could be locally detrimental to seal integrity depending on the strain accommodation behaviour of the formation.

A recent CSIRO-VicDPI collaborative research program investigates the impact of deformation on the integrity of the regional top seal, Lakes Entrance Formation. This study depends on multiple geological parameters calibrated by the naturally occurring hydrocarbon leakage and seepage indicators reported by Goldie-Divko et al. (2010). Among these parameters, volume of shale (V_{sh}) and fracture density were constrained by significant input from seismic inversion and attributes and are found related to the top seal efficiency. We present here the main workflow used in the derivation of the Vsh and fracture density parameters with the aid of 2D and 3D seismic surveys.

METHOD AND RESULTS

An important factor in top seal efficiency is the spatial variation of its shale content (Vsh) as it (i) controls the permeability and containment efficiency; (ii) impacts on brittleness and affects fault development; and (iii) controls the shale gouge ratio (SGR) of the fault rocks and their membrane seal capacity.

Near 50 samples from the Lakes Entrance Formation were quantitatively analysed using automated mineral analysis (AMA) method (Goldie-Divko et al., 2010) that provided fraction of the mineral constituents that can be turned into Vsh (Figure 2B). The Vsh was also computed based on the calibrated gamma ray index using the gamma ray logs of 76 wells (Figure 2C). Although well density is high in the Central Deep, allowing to capture spatial variation confidently, the Southern Platform and Southern Terrace is intersected by only a dozen wells that are probably insufficient to reveal the first order trends.

In order to achieve a better coverage for this part of the basin, we estimate Vsh based on multi attribute analysis and inversion of seismic data using a 2010 2D seismic survey. 8 lines that are closely located to at least one well were selected from the survey with amplitude preserved, time migrated data volumes (Figure 2C). At each well location, composite seismic amplitude and acoustic impedance traces were constructed within the radius of 3 CDPs in order to relate the seismic data to the well derived reference Vsh data. Using a multi-attribute regression analysis, a transformation was established from seismic attributes (time integrated absolute amplitude and amplitude envelope) and impedance to Vsh. Using the transformation, Vsh pseudo traces were computed at each seismic trace which provided a vertical Vsh profile at the trace locations along the selected seismic lines (Figure 2C). Then, the Vsh samples corresponding to the Lakes Entrance Formation on each trace was averaged to achieve a formation mean that was integrated with the well-derived Vsh data set.

A final Vsh model for the top seal was created by a stochastic simulation based on the well data over the background of average Vsh distribution (Figure 2C) with some conditioning effect from the AMA derived Vsh (Figure 2B). The resulting model captures the first order trend with a more textured distribution pattern (Figure 2D). It shows the Vsh transitioning from the central deep with values around 50% to the southern terrace and southern platform with values as low as 10%. On the southern terrace and southern platform there is an increasing trend to the east with Vsh around 40% and up to 50% in the more offshore area.

The top seal efficiency is also related to mechanical integrity of the seal which could be undermined by faults. The localized, large scale fault systems can be interpreted and mapped with some confidence using 2D and 3D seismic surveys to evaluate for their potential impact on the top seal efficiency. However, there are also small-scale faults distributed throughout the basin which are resolvable in seismic data but cannot be manually interpreted and mapped at the regional scale of this study. As a result, the seismic attributes and an automated fault picking algorithm was used in order to account for this small-scale distributed deformation.

Spectral blueing (Lancaster and Whitcombe, 2000) was applied to the 2010 2D seismic survey to generate a higher resolution reflectivity dataset. A matching filter (blueing operator) is designed that shapes the post-stack seismic amplitude spectrum to resemble the amplitude spectrum of measured logs (25 wells used). This resulted in increasing the amount of high frequencies in seismic data, while noise is kept to an acceptable level. Spectral blued sections usually reveal more information about the subsurface increasing the imaging and resolution of geobodies (Kazemeini et al., 2010) or small scale faulting. The high resolution data was then filtered to improve fault detection using a workflow modified from dGB Earth Science (Friso Brouwer, personal communication).

A meta-attribute that sharpens the faults and suppresses non-fault discontinuities was designed by integrating similarity attributes, median dip filter and diffusion filter (dGB, 2012). The filtered high resolution seismic data was then used to detect faults based on the similarity attributes (Figure 3C). This results in the definition of all faults with offsets approaching the seismic resolution (c. 10m) that was used to produce a fault density map for the lake Entrance Formation over the 2010 2D seismic survey (Figure 4B). This density map was integrated with a fault density map from the 3D mega survey (Figure 4A) and yielded a normalised fault density map for the Lake Entrance Formation for the Southern Platform, the Southern Terrace and the western Central Deep (Figure 4C). The final density map illustrates the most intensely faulted areas of the top Lakes Entrance Formation over the southern flank.

Higher fault density areas are present (i) in the southern Central Deep, mostly due to polygonal faulting (Figure 3A, B and Figure 4A), (ii) over the central Southern Terrace and (iii) over the central and south-eastern Southern Platform. The normalised fault density map is probably composite not only capturing the density of small scale and polygonal faults but also capturing the deformation of larger faults. The latter is probably more influential on the 2D derived data set where the large offset faults with wider deformation zone are represented by larger number of faults. This is expected because larger deformation zones are likely to be structured by increased number of small-scale faults.

CONCLUSIONS

This study provides a basin-scale first-order estimates of the V_{sh} and fracture density distribution of the Lakes Entrance Formation along the southern flank of the Gippsland Basin. These parameters are potentially influential on the seal efficiency of the formation. This is evidenced by the general correlation of naturally occurring hydrocarbon leakage and seepage indicators over the domains of low V_{sh} (Figure 2D). The correlation is stronger in the case of fracture density high fracture density where seven out of nine leakage indicators are distinctly located over elevated fracture densities in the coverage area (Figure 4C).

ACKNOWLEDGMENTS

The authors wish to thank dGB Geosciences and CGGVeritas for providing software licenses and support.

REFERENCES

dGB, 2012, Fault Enhancement Filtering: http://www.opendtect.org/index.php/support.html.

Goldie Divko, L. M., O'Brien, G. W., Harrison, M. L., Hamilton, P. J., 2010, Evaluation of the regional top seal in the Gippsland Basin; implications for geological carbon storage and hydrocarbon prospectivity: APPEA Journal 2010, 50, 463-486.

Kazemeini, S.H., Yang, C., Juhlin, C., Fomel, S. And Cosma, C., 2010, Enhancing seismic data resolution using the prestack blueing technique: An example from the Ketzin CO2 injection site, Germany: Geophysics,vol. 75, 6, v101–v110.

Lancaster, S. and Whitcombe, D. 2000, Fast track spectral blueing, SEG Meeting 2000, Calgary, Abstract.

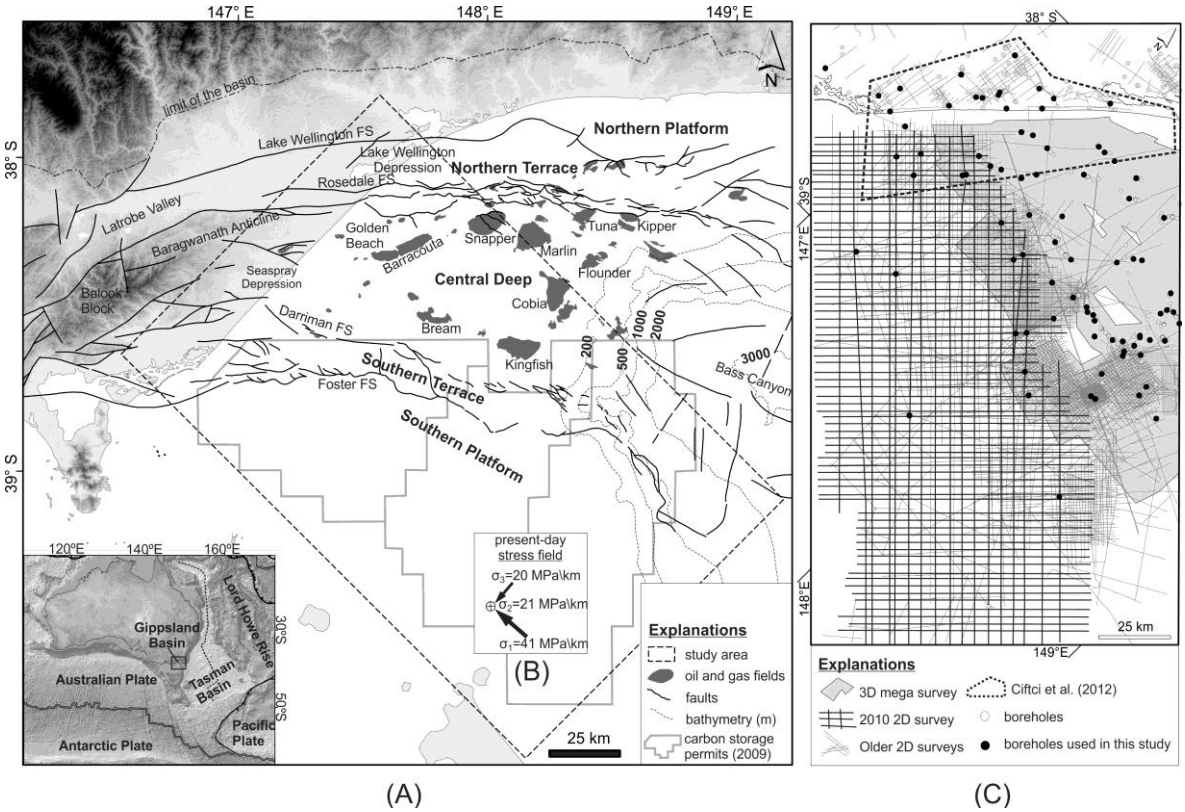

Figure 1. (A) Map of the Gippsland Basin showing the boundaries of the study area, the main fault systems and the basin compartments, the major oil and gas fields and the carbon storage permits released in 2009; (B) Present-day stress tensor in the basin (Table 1); and (C) The available subsurface data set in the study area. The location of (C) is illustrated in (A) as the dashed rectangle.

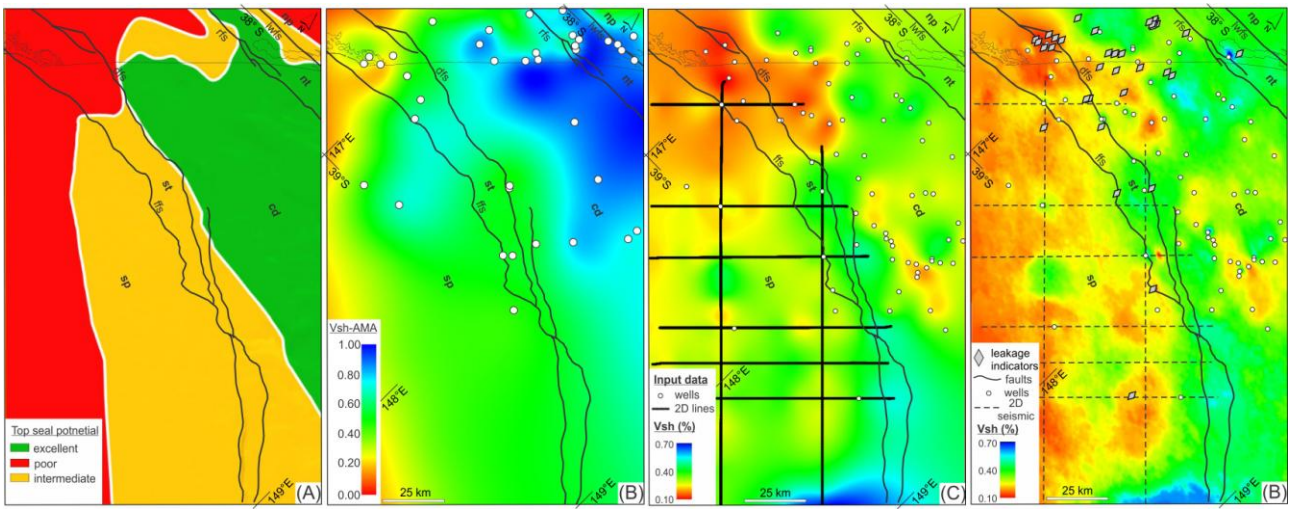

Figure 2. Maps of the Lakes Entrance Formation showing: (A) Top seal potential; (B) Vsh distribution based on automated mineral analysis (AMA). Dots illustrate the location of the samples; (C) Average Vsh distribution of the formation based on gamma ray logs from wells and seismic inversion from number of 2D seismic lines. High level of smoothing is applied to the map to eliminate bullseyes and achieve a general trend; and (D) The final Vsh model of the formation with stochastic

simulation based on the background trend in (C) and well derived Vsh. Abbreviations: ffs – Foster Fault System; dfs – Darriman fault System; rfs – Rosedale Fault System; lwfs – Lake Wellington Fault System; sp – Southern Platform; st – Southern Terrace; cd – Central Deep; nt – Northern Terrace; np – Northern Platform.

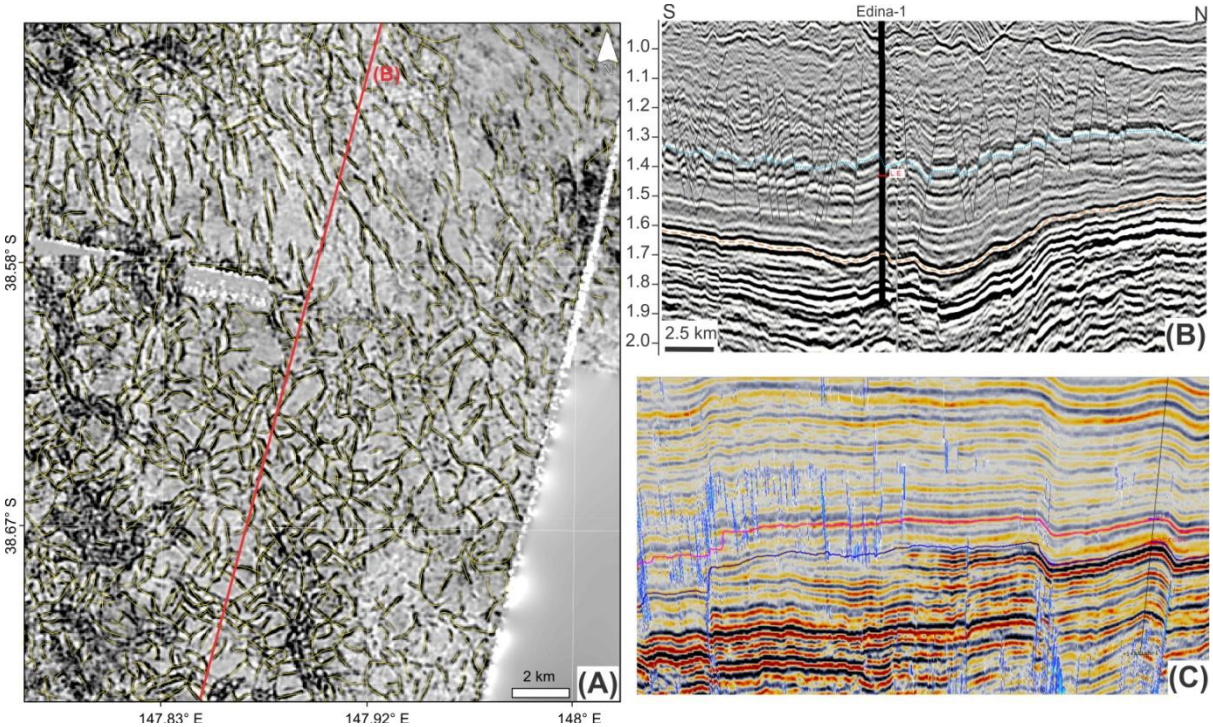

Figure 3. (A) Similarity map of the top Lakes Entrance Formation showing the pattern of intense polygonal faulting. Red line illustrates the location of the seismic profile in (B). See Figure 4A for the location of the map; (B) A seismic profile depicting the deformation pattern of polygonal faults in cross section. Blue line is the top Lakes Entrance Formation and the dashed orange line is the top Latrobe unconformity; and (C) Automated fault picking applied to blued and filtered seismic. Blue lines represent the faults and red horizon is the approximate top Lakes Entrance Formation.

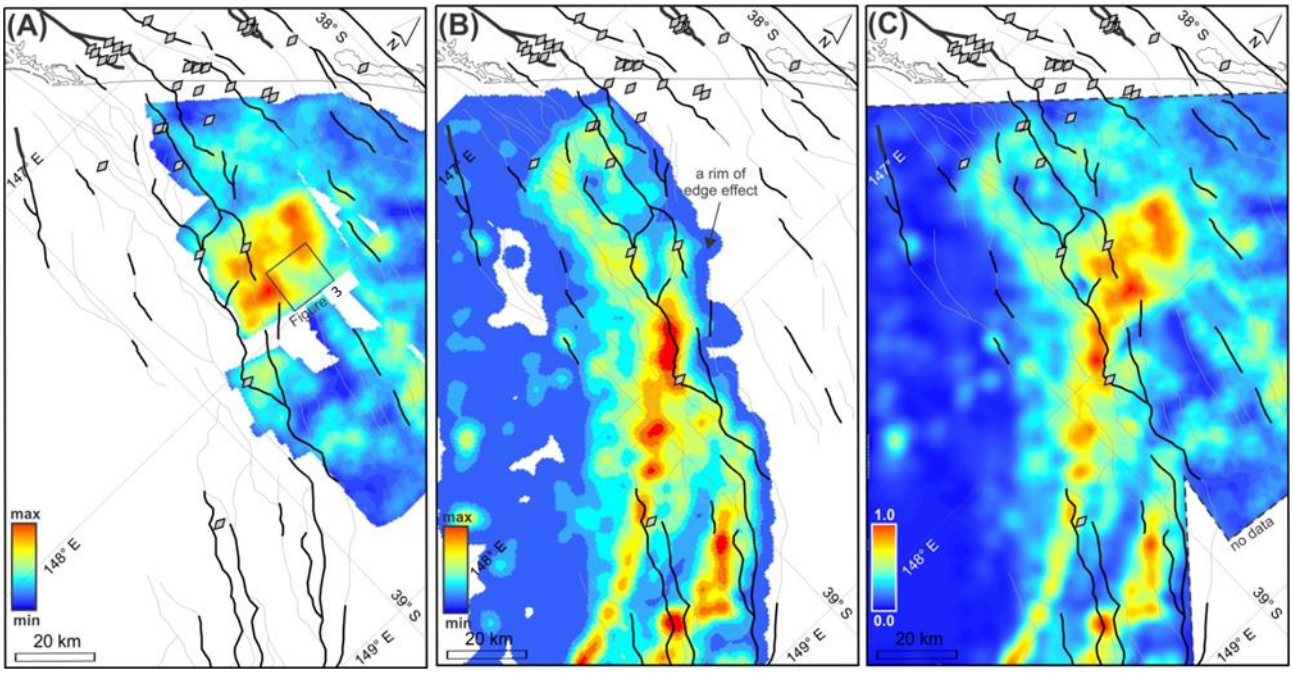

Figure 4. Fault density maps. (A) Line density map based on automated fault mapping form the top Lakes Entrance Formation across the 3D mega survey. The black square shows location of the similarity map in Figure 3A; (B) Point density map based on the automated fault mapping from 2D seismic sections of the 2010 survey (Figure 3C); and (C) Merged fault density map rescaled between 0 (minimum) and 1 (maximum). Dashed lines depict the approximate limits of the data and boundary of the map